Faculty of Technology, Design & Environment
School of Engineering, Computing & Mathematics

Assessment cover

Module No:	ENGR7006	Module title:	Advanced Vehicle Aerodynamics

Assessment number:	**1**	Assessment title:	**Individual Portfolio**

Banner assignment identifier	*CWS1WEEK9*	Due date and time**:**	17:00hrs Friday 22nd November 2024, Week 9.

Estimated total time to be spent on assignment:	*30 hours per student*

LEARNING OUTCOMES

On successful completion of this assignment, students will be able to achieve the following learning outcomes (LOs): *LO numbers and text to be copied and pasted from the module handbook*
LO 1: Evaluate ground vehicle design features, associated flow structures and vehicle performance characteristics using a range of communication methods.
LO 3: Critically evaluate aerodynamic performance data output from experimental testing and numerical modelling of ground vehicles using a range of communication methods.
LO 4: Predict and compare boundary layer characteristics.

Engineering Council AHEP4 LOs assessed (from S1 2024 Onwards) *LOs copied and pasted from the AHEP4 matrix (add rows as required)*	
LO number	**LO text**
M3	Select and apply appropriate computational and analytical techniques to model complex problems, discussing the limitations of the techniques employed
M4	Select and critically evaluate technical literature and other sources of information to solve complex problems
M17	Communicate effectively on complex engineering matters with technical and non-technical audiences, evaluating the effectiveness of the methods used
M18	Plan and record self-learning and development as the foundation for lifelong learning/CPD

Statement of Compliance

By submitting this assessment I declare that the work submitted is my own and that the work I submit is fully in accordance with the University regulations regarding assessments.
(*www.brookes.ac.uk/uniregulations/current*)

Use of AI Tools: You are required to use this form to declare which AI tools you have used and how you have used them. Please complete the form and attach it to your submission as an Appendix, if you have used such tools.

Index

Figure Content

Table Content

Vehicle Performance Evaluation

Input data acquired from automobile-catalog.com				
Nissan Skyline R34 GTT				
Vehicle data	Symbol	Units	Value	Value
Curb weight (without driver)	m	kg -> N	1,450	14,224.5
Mass moment of inertia	mres	factor -> kg	1.30	1,885
Rolling coefficient	μr	factor -> kg	0.01	14.50
Wheelbase	L	m	2.67	
L1 from CoG to front axle	L1	m	1.60	
Horsepower	hp	hp -> Watts	197	144,893.50
Drag coefficient	Cd	Cd	0.33	
Frontal area	A	m^2	1.93	
Air density	ρ	kg/m^3	1.23	

Table 1. Input metrics for the vehicle performance evaluation

Maximum speed

To find the maximum speed of the vehicle, we find the total resistance of the vehicle and compare it with the power output of the vehicle.

At a slope of 0 degrees, at 245km/h, the $F_{Total} = 2096$ N, achieving the maximum power output. The impact of the aerodynamic performance becomes important after 70km/h, but it is not until we achieve the tallest gear, when the aerodynamic resistance becomes the primary resistance.

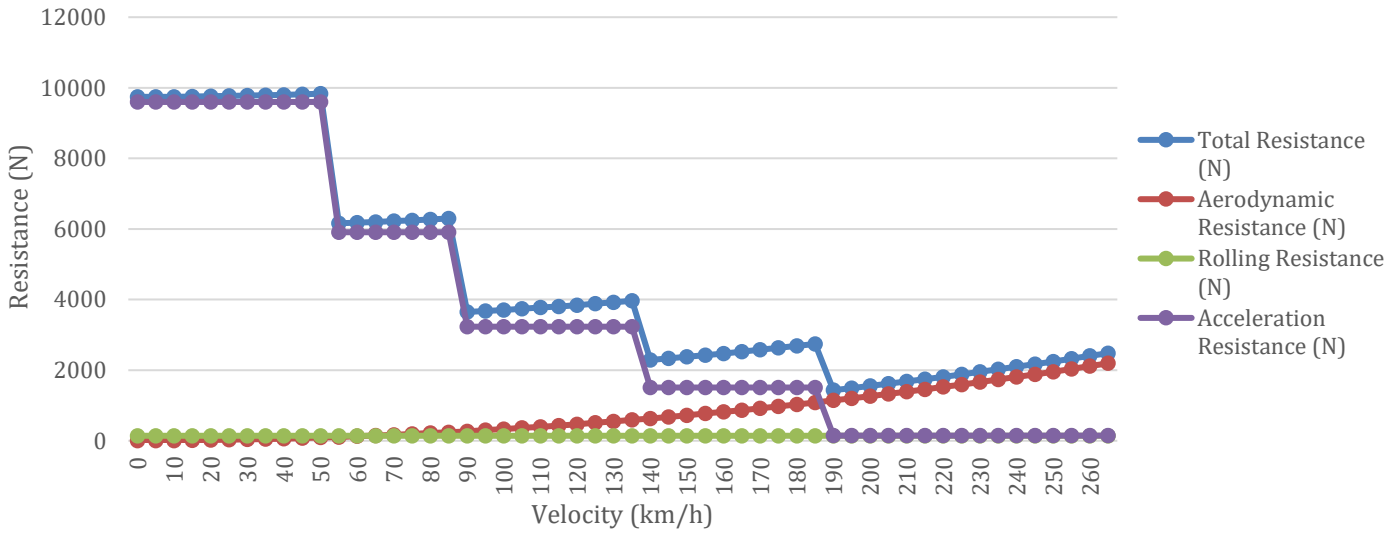

Figure 1. Total resistance for a vehicle at different velocities

We can also find the maximum velocity utilizing the formula (Milliken, 1994):

$$v = \sqrt[3]{\frac{2.\eta.P_{max}}{\rho.A.C_D}} = \sqrt[3]{\frac{2 * 0.9 * 197hp}{1.225 * 1.93 * 0.33}} = 69.4m/s = 249km/h \approx 245km/h$$

Elasticity

To find the effects of aerodynamic performance on vehicle elasticity, we modify the drag coefficient, simulating different bodyworks, obtaining then the 60-120km/h time for the vehicles on the second to last gear, as that is the direct gear for this transmission.

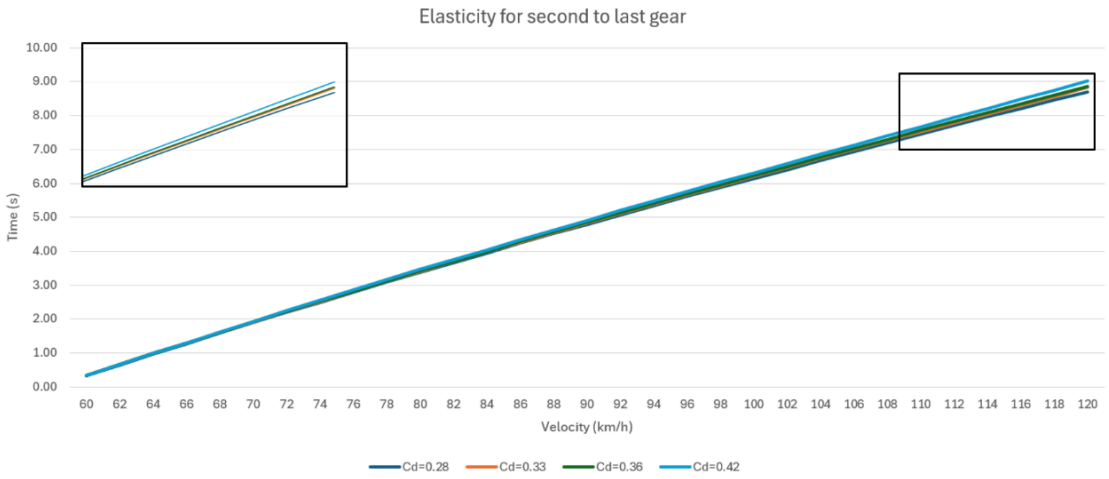

Figure 2. Elasticity 60-120km/h for direct gearing

We can observe that, to achieve the same acceleration, the vehicles with more drag would need to output more torque in order to overcome it at the same time.

Acceleration

To find the effects of aerodynamic performance on vehicle acceleration, the acceleration is assumed to be an average over a whole gear; ideally, it would follow a non-linear downward curve. As aerodynamic resistance grows parabolically when velocity increases, the vehicle requires more torque to overcome it, thus slowing the vehicle's acceleration.

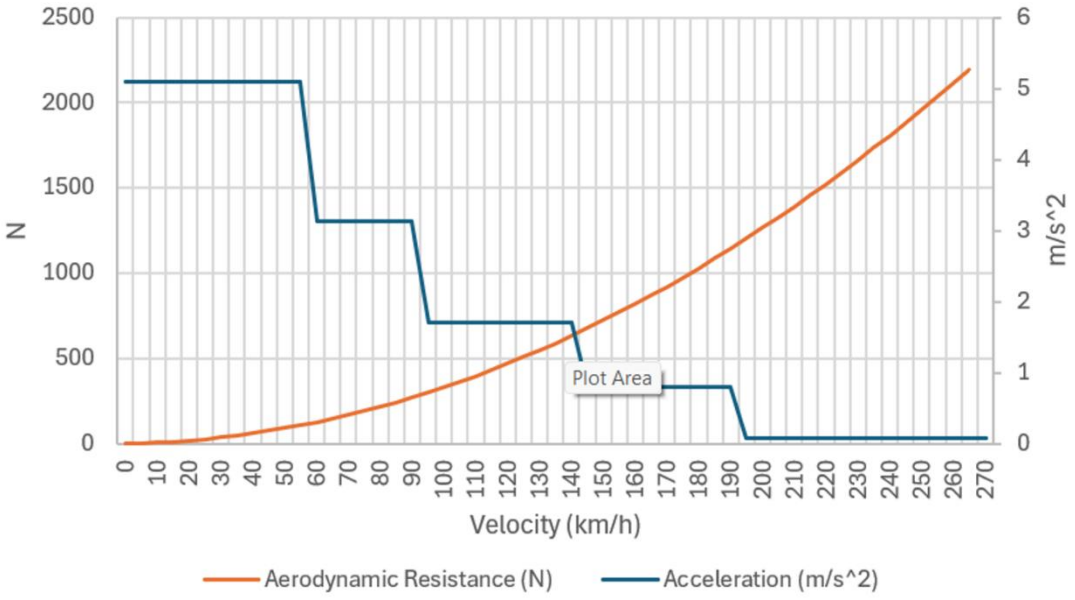

Figure 3. Effects of aerodynamic performance on vehicle acceleration capacity

If we vary the vehicle bodywork again, we can see that the acceleration of the vehicle slows down earlier as the coefficient grows.

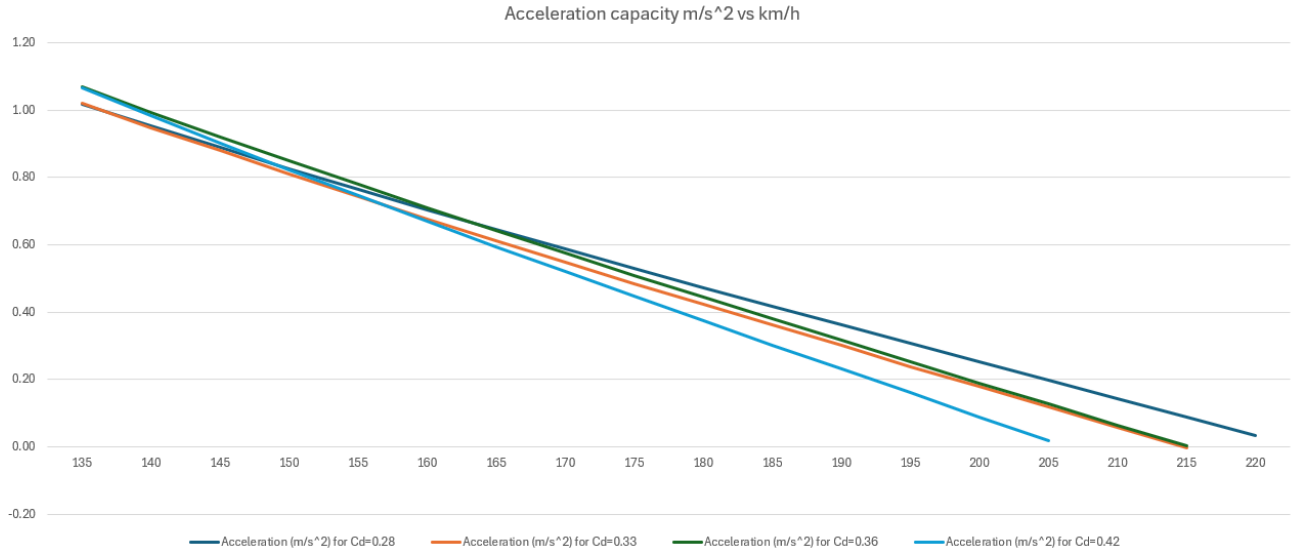

Figure 4. Effects of drag coefficient changes on vehicle acceleration performance

Power Absorbed in Aerodynamic Drag

For this vehicle, the amount of power absorbed by the aerodynamic resistance becomes greater than the power outputted by the engine at 258km/h.

Nissan Skyline R34 GTT

Frontal area (m^2)	Cd	Air density (kg/m^3)	Power Output (bhp)	$F_{D,total} = \frac{1}{2} * \rho * C_d * A_{frontal} * V^2$
1.93	0.33	1.225	197	

Velocity (km/h)	Power Absorbed in Aerodynamic Drag (N)	Power Absorbed in Aerodynamic Drag (bhp)
260	2034.787384	199.8053931
259	2019.165274	197.508802
258	2003.603365	195.2298769
257	1988.101656	192.9685496
256	1972.660148	190.7247518
255	1957.278841	188.4984155
254	1941.957735	186.2894723
253	1926.69683	184.097854
252	1911.496125	181.9234925
251	1896.355621	179.7663196
250	1881.275318	177.6262669
245	1806.776816	167.1804214
240	1733.783333	157.1523529
235	1662.294871	147.5335353
230	1592.311429	138.3154425
225	1523.833008	129.4895486
220	1456.859606	121.0473274
215	1391.391225	112.9802528
210	1327.427865	105.2797989
205	1264.969524	97.93743954

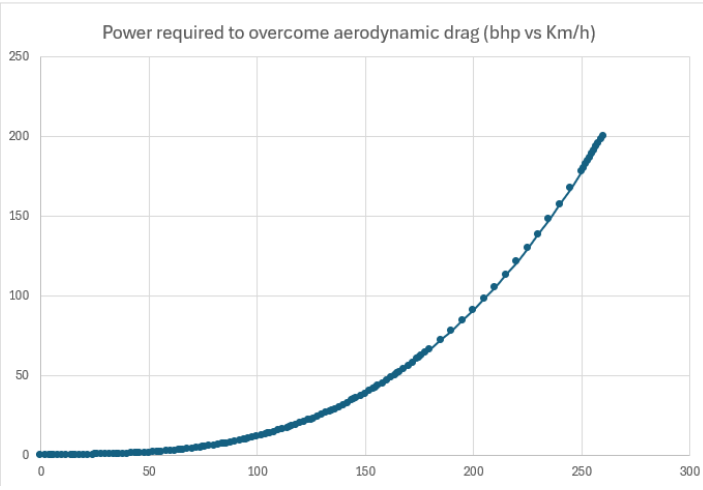

Figure 5. Power absorbed by drag force

Impact of yaw

Yaw has a negative impact on the performance, adding the effect of side force to the drag coefficient, $C_{D_i} = C_D * cos\alpha + C_Y * sin\alpha$, increasing the overall drag, reducing the vehicle top speed. We can see this effect graphically on the power absorbed by the aerodynamic resistance:

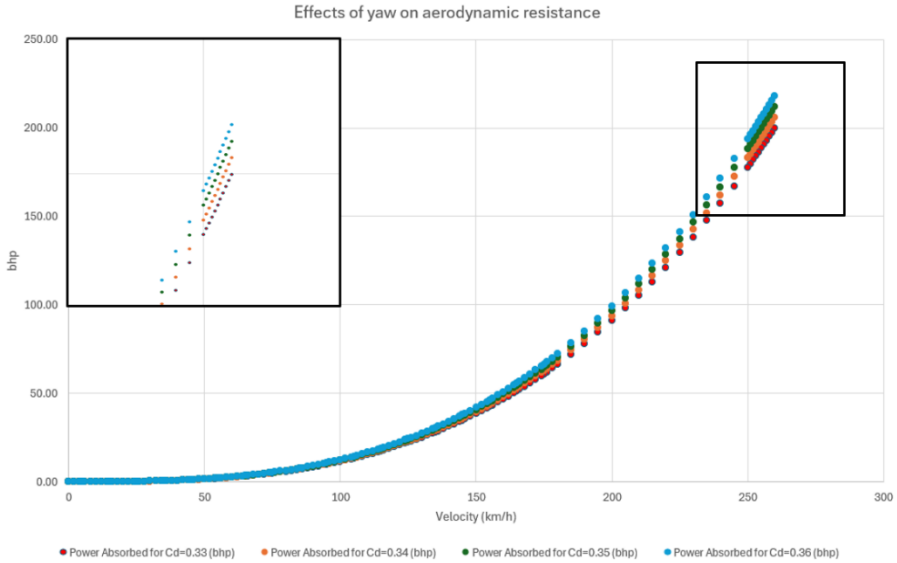

Figure 6. Impact of yaw on vehicle acceleration and maximum velocity performance

Analysing the results, we can see that, for every variation of 0.01 to the Cd, the maximum speed of this vehicle will get modified by 0.8%.

Velocity (km/h)	Power Absorbed for Cd=0.33 (bhp)	Power Absorbed for Cd=0.34 (bhp)	Power Absorbed for Cd=0.35 (bhp)	Power Absorbed for Cd=0.36 (bhp)	Cd variation influence on speed
260	199.81	205.86	211.91	217.97	
259	197.51	203.49	209.48	215.46	
258	195.23	201.15	207.06	212.98	
257	192.97	198.82	204.66	210.51	
256	190.72	196.50	202.28	208.06	0.78%
255	188.50	194.21	199.92	205.63	
254	186.29	191.93	197.58	203.22	
253	184.10	189.68	195.26	200.83	1.19%
252	181.92	187.44	192.95	198.46	
251	179.77	185.21	190.66	196.11	0.80%

Table 2. Variation of drag coefficient effect on maximum velocity performance

Boundary Layer Evaluation for the OBU Wind Tunnel

For the OBU wind tunnel:

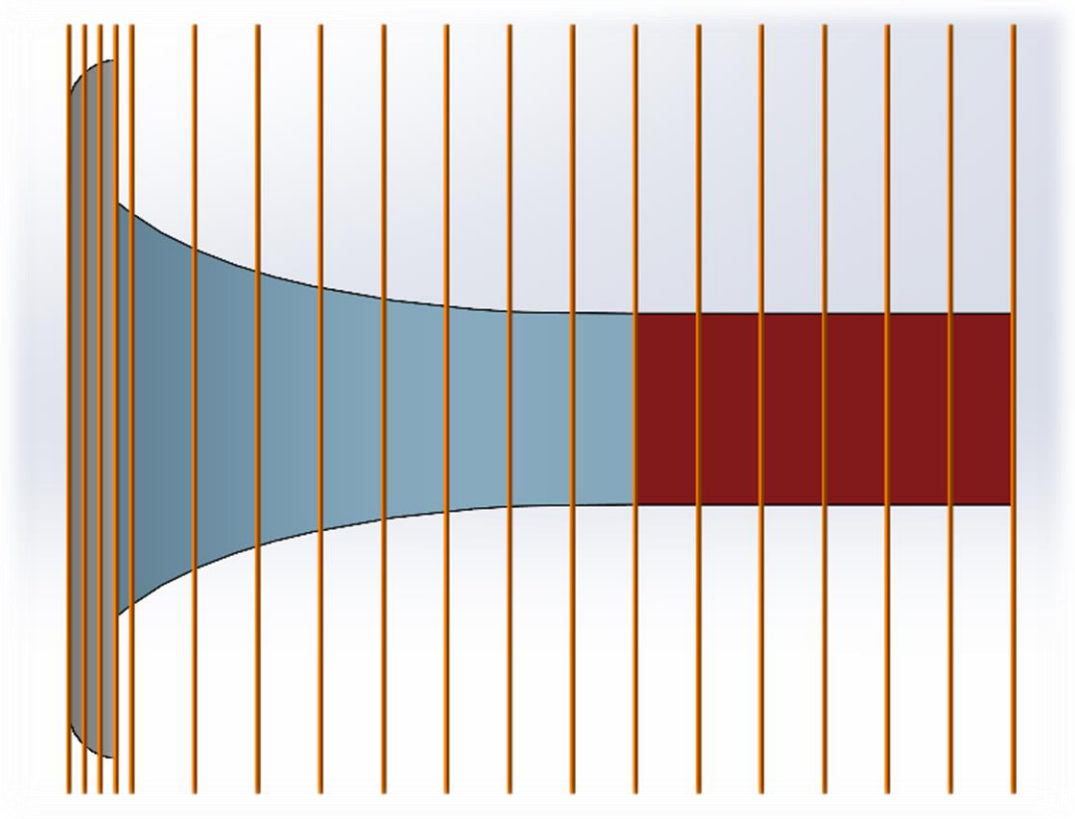

Figure 7. OBU Wind tunnel inlet (blue) and working area (red) measurement locations

Assuming that the flow is steady and uncompressible, with smooth walls, no vibrations and not considering the transient state of the fluid, while making use of the formulas for the various thickness (Hucho, 2013):

	Laminar flow	Turbulent flow
Boundary Layer Thickness	$\delta = \frac{4.91 * X}{\sqrt{Re_x}}$	$\delta = \frac{0.16 * X}{Re_x^{1/7}}$
Displacement Thickness	$\delta^* = \frac{1.72 * X}{\sqrt{Re_x}}$	$\delta^* = \frac{0.020 * X}{Re_x^{1/7}}$
Momentum Thickness	$\theta = \frac{0.664 * X}{\sqrt{Re_x}}$	$\theta = \frac{0.016 * X}{Re_x^{1/7}}$

Table 3. Formulas for the different thickness

Reynolds number is obtained with the formula: $Re_x = \frac{V * D_H}{\nu}$, where Re_x<3.5E+05 is considered laminar flow, Re_x>5E+05 is considered turbulent flow, and the transient state is treated as laminar flow.

V=maximum velocity for the section, D_H=Hidraulic diameter, where, $D_H = L$, and ν=Kinematic viscosity, for an air temperature of 19ºC, ρ $= 1.2\, kg/m^3$ and $\nu = 1.507e-5\, m/s^2$, we find that:

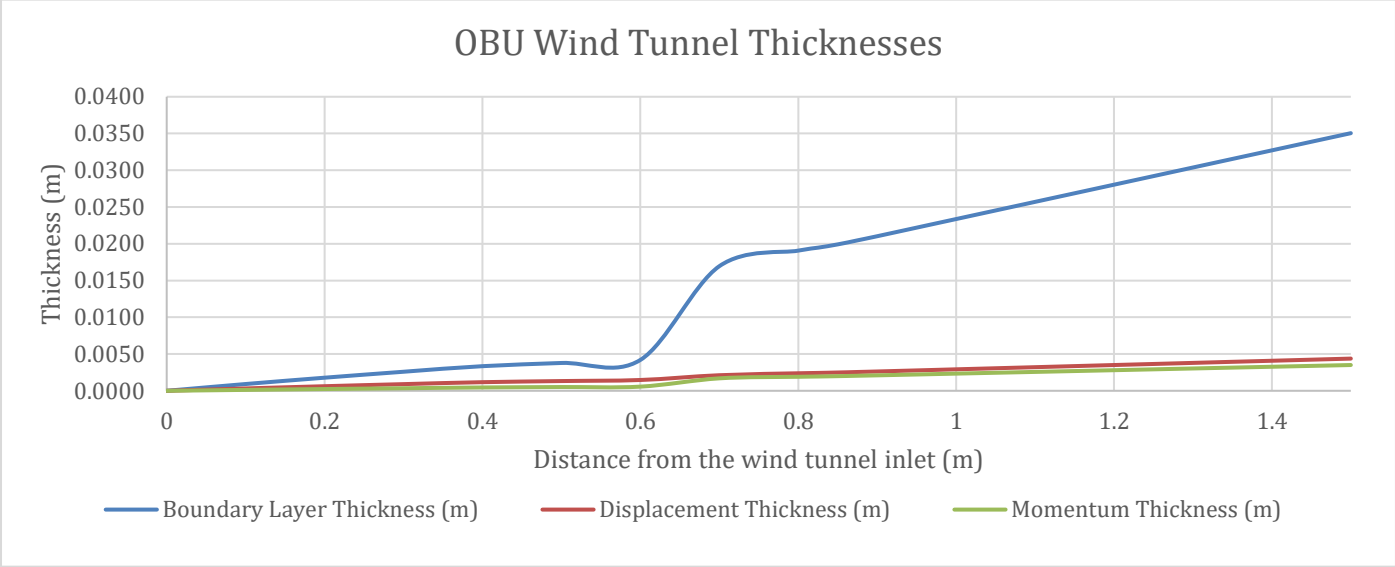

Figure 8. OBU Wind Tunnel different thicknesses

	Origin (m)	Reynolds number	Turbulent	Boundary Layer Thickness (m)	Displacement Thickness (m)	Momentum Thickness (m)
	0	2.259E+05	Laminar	0.0000	0.0000	0.0000
	0.1	2.839E+05	Laminar	0.0009	0.0003	0.0001
	0.2	3.040E+05	Laminar	0.0018	0.0006	0.0002
	0.3	3.232E+05	Laminar	0.0026	0.0009	0.0004
	0.4	3.440E+05	Laminar	0.0033	0.0012	0.0005
	0.5	4.209E+05	Transient	0.0038	0.0013	0.0005
	0.6	4.923E+05	Transient	0.0042	0.0015	0.0006
	0.7	5.503E+05	Turbulent	0.0169	0.0021	0.0017
	0.8	6.132E+05	Turbulent	0.0191	0.0024	0.0019
	0.825	6.584E+05	Turbulent	0.0195	0.0024	0.0019
	0.85	6.924E+05	Turbulent	0.0199	0.0025	0.0020
	0.875	7.014E+05	Turbulent	0.0205	0.0026	0.0020
	0.9	7.060E+05	Turbulent	0.0210	0.0026	0.0021
Working Area	**0.95**	7.060E+05	Turbulent	0.0222	0.0028	0.0022
	1	7.060E+05	Turbulent	0.0234	0.0029	0.0023
	1.1	7.060E+05	Turbulent	0.0257	0.0032	0.0026
	1.2	7.060E+05	Turbulent	0.0280	0.0035	0.0028
	1.3	7.060E+05	Turbulent	0.0304	0.0038	0.0030
	1.4	7.060E+05	Turbulent	0.0327	0.0041	0.0033
	1.5	7.060E+05	Turbulent	0.0350	0.0044	0.0035

Table 4. Results table for OBU wind tunnel boundary layer information

Boundary Layer Thickness:

From the boundary layer thickness, we can see observe where we would need to locate a body in order for it to be in contact with free-stream flow, allowing for better behaviour data collection. In the case of the OBU wind tunnel, we can that the body we intend to experiment with needs to be at least between 0.02m and 0.035m of the walls, depending on the position along on the working area.

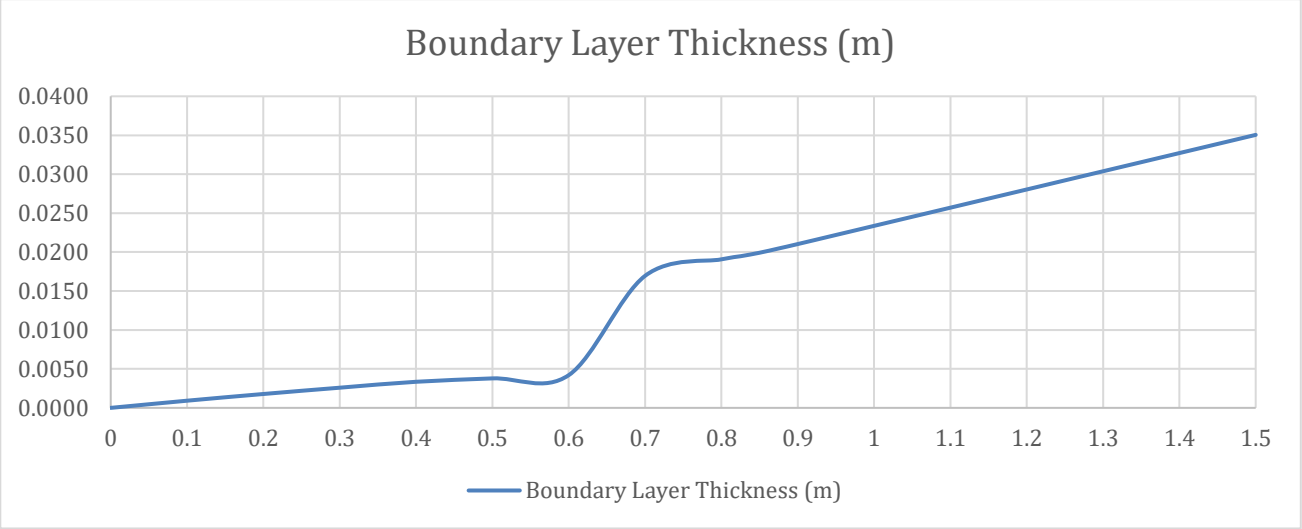

Figure 9. Boundary layer thickness for OBU wind tunnel

Boundary Layer Displacement Thickness:

Displacement thickness refers to the degree to which the airflow is disturbed by the boundary layer surrounding the test object; larger values mean that the boundary layer is thicker, which in turn means that the airflow around the object is more disturbed, resulting in less accurate lift and drag values.

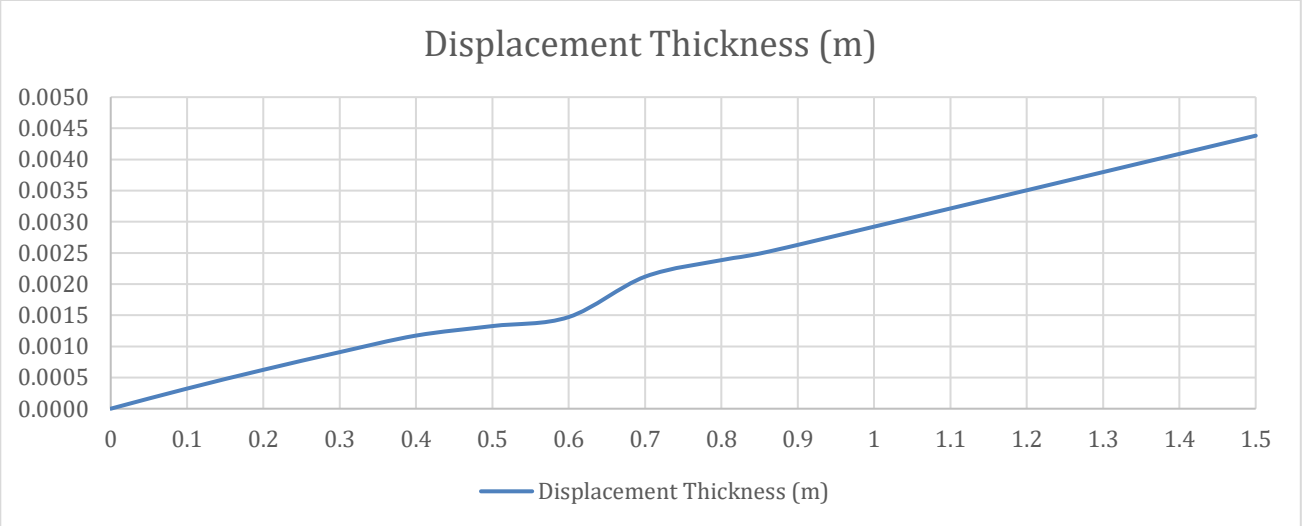

Figure 10. Displacement thickness for OBU wind tunnel

Boundary Layer momentum thickness:

Momentum thickness is a length scale representation that amounts for the momentum loss given due to the friction between a fluid and a surface. This represents the distance from the surface on which the fluid is slowed down.

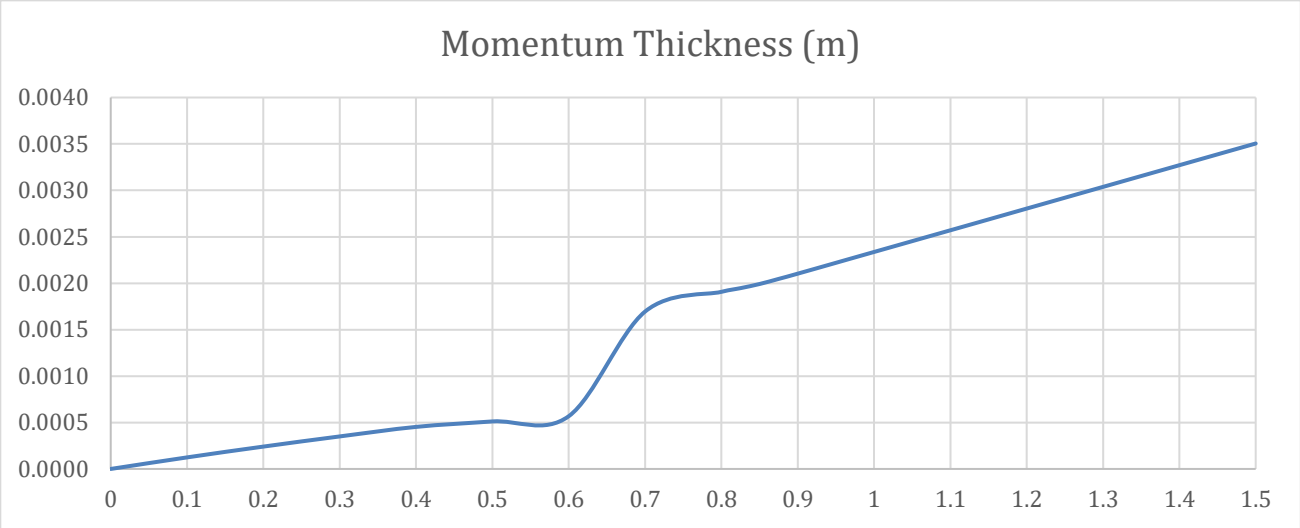

Figure 11. Momentum thickness for OBU wind tunnel

We can interpret from the graphs that the closer we are to the start of the working area, the less obstructions we will get, but, as we need data before the fluid reaches the test object, especially to analyse free flow conditions, we need to compromise the position of the test object by placing it at a certain distance from the origin, where the measuring device and the test object do not disturb each other.

Body Shape Aerodynamic Impact and Stability

Flow fields refer to how the air interacts with a vehicle body, vortex generation, drag impact and aerodynamic efficiency.

Flow fields associated with different body variants

Here we can visualize the effects on surface pressure of different underbody types for the DrivAer model:

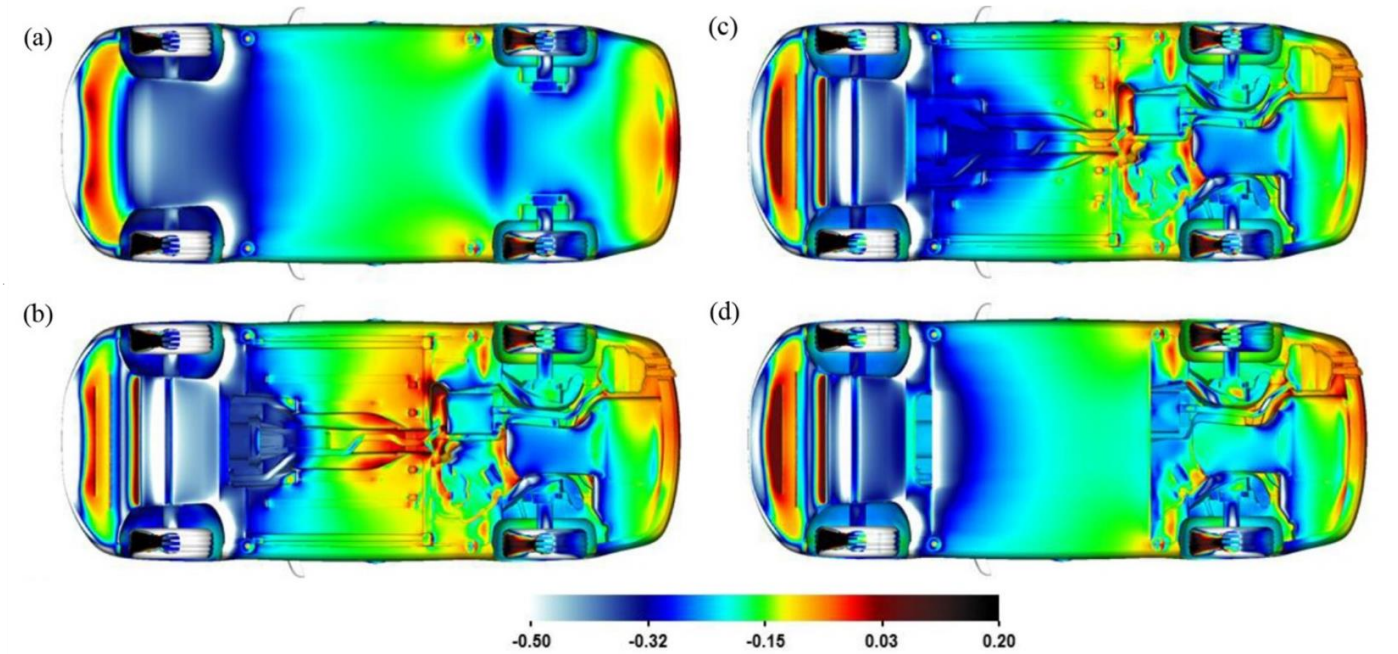

Figure 12. Static pressure from PowerFLOW simulation along the underbody variants

Here we can visualize the effects of different rear body shapes for the DrivAer model on air velocity along the center line of the vehicle:

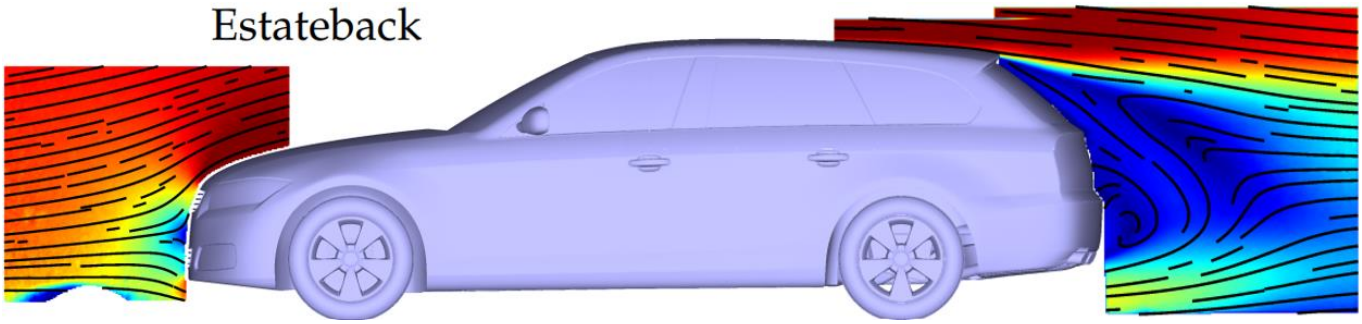

Figure 13. Side profile for PIV plane of normalised velocity magnitude for Estateback DrivAer model

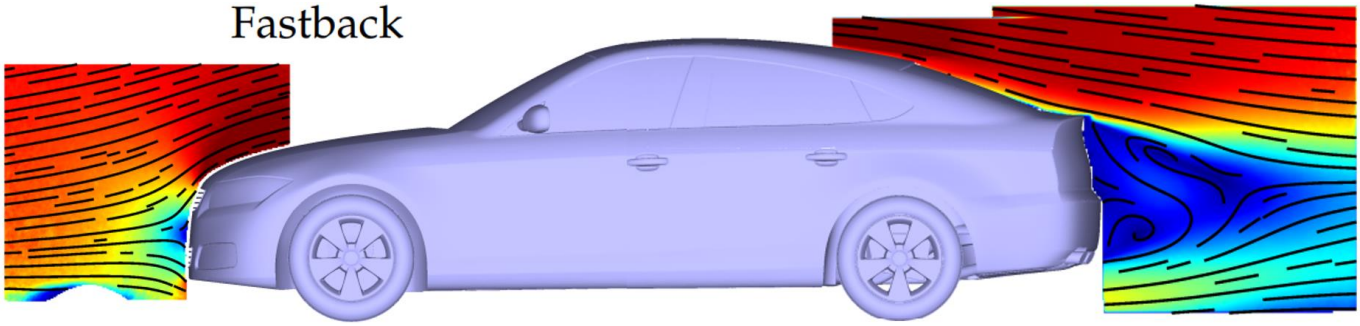

Figure 14. Side profile for PIV plane of normalised velocity magnitude for Fastback DrivAer model

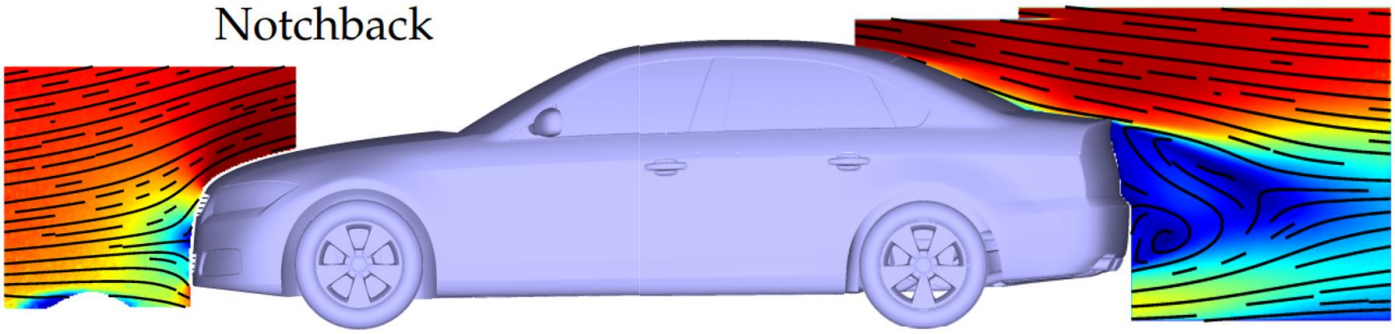

Figure 15. Side profile for PIV plane of normalised velocity magnitude for Notchback DrivAer model

From these simulations we confirm that the smoothest the underbody, the smallest the lift will be, as in experiment a), we see the most stable flow and the lowest overall pressure.

Impact on Cd and Cl

Of the different bodyworks, we see that the Estateback presents the largest wake and Cd, due to the bluff body, resulting in a less sharp rear. Although the Fastback and Notchback present similar wakes and drag coefficients, due to the rear windscreen position of the Notchback, the Fastback has a sharper edge, achieving a smaller separation, thus presenting a smaller wake and better aerodynamic efficiency.

Vehicles with smoother underbodies reduce lift due to more stable flow, improving overall performance.
The rear body shape has a great effect on drag, as an Estateback increases drag due to larger wakes, while improving downforce.
Sharp-edged designs like the Fastback or the Notchback minimize separation, reducing drag and improving aerodynamic efficiency, but implicating more lift.

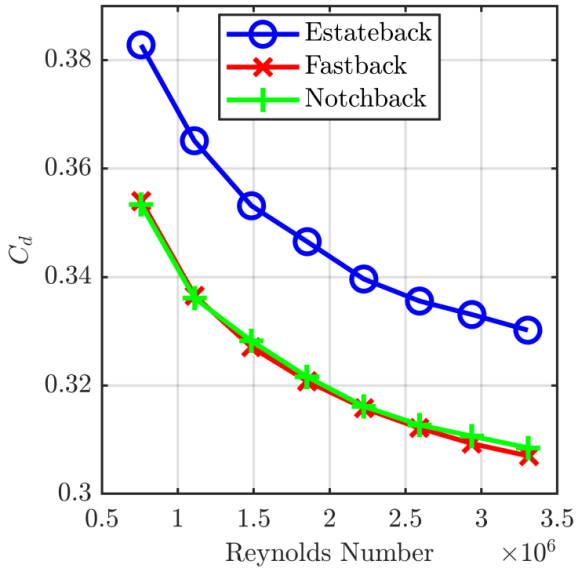

Figure 16. Reynolds sweep for the drag coefficient for each DrivAer geometry

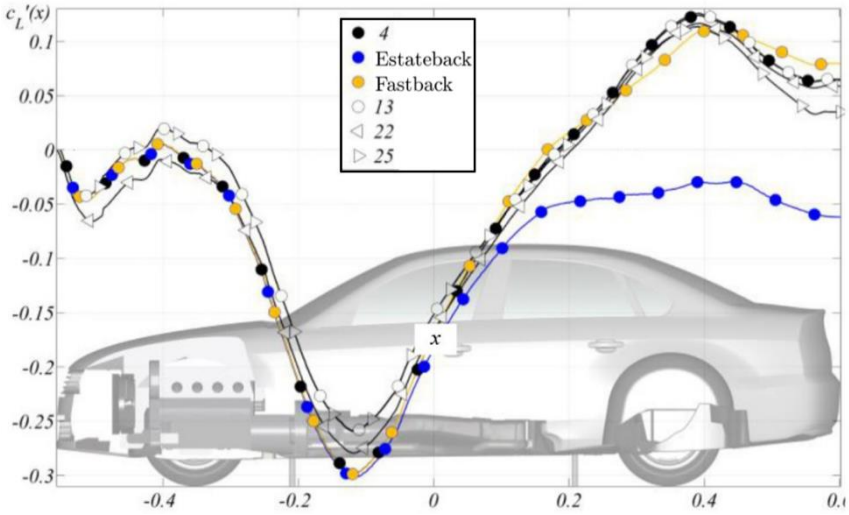

Figure 17. Lift development along the different bodywork models

Instability solutions

Instability is produced when a vehicle receives lateral forces, usually during yawing or passing. To optimize stability, some methods used include:

- The implementation of sharp edges on the front and rear edges of the vehicle, in order to reduce front lift and rear wake, improving aerodynamic drag and downforce generation.

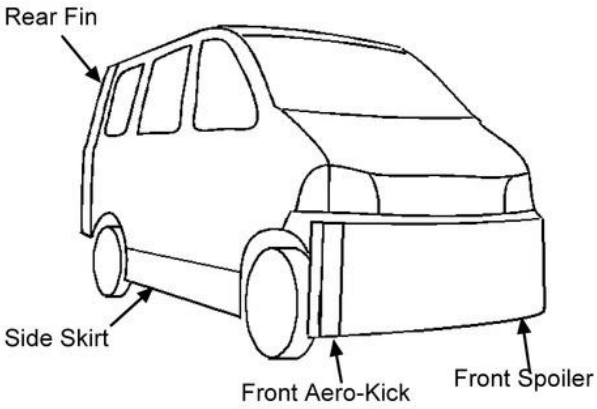

Figure 18. Sharp-edge additions to CAD simulation model

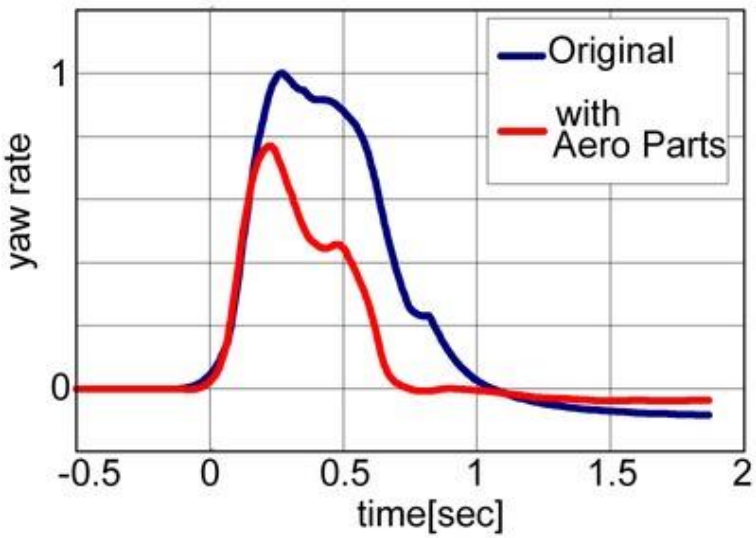

Figure 19. Effect on yaw rate by CAD simulation model

- Adding front downforce or rear lift, in order to prevent take-off in case the vehicle encounters extreme cases of nose pitch when on a steep slope.

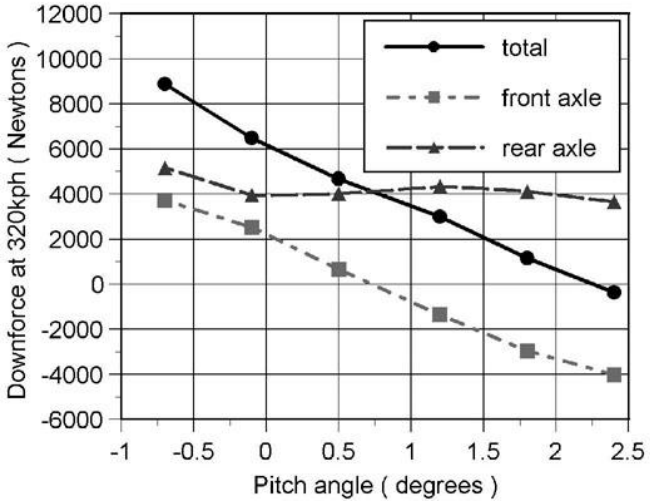

Figure 20. The effect of chassis pitch upon downforce when pivoted about the rear axle

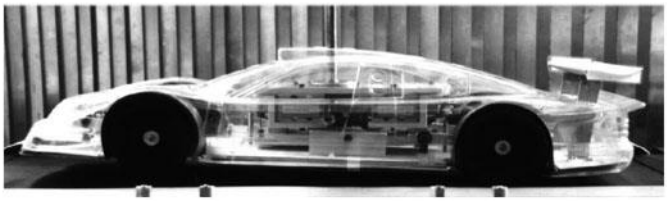

Figure 21. Effects of pitch angle model at +2.5 degrees incidence

- Including lateral bleed and strakes on the vehicle design; these has been proved to reduce the effects yawing has on the vehicle performance, maintaining stability for larger yaw angles, without displaying a negative effect on drag at 0 yaw.

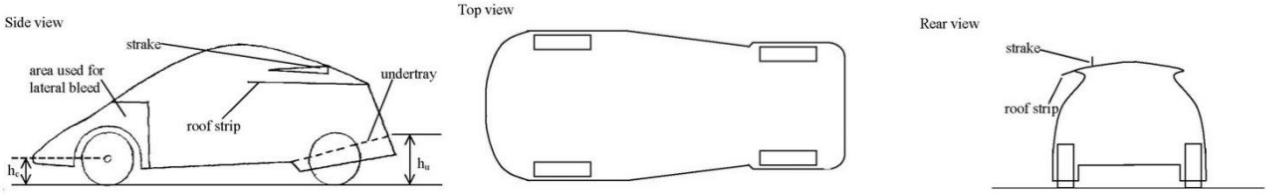

Figure 22. Drawings showing the shape of the model with roof strips and strakes

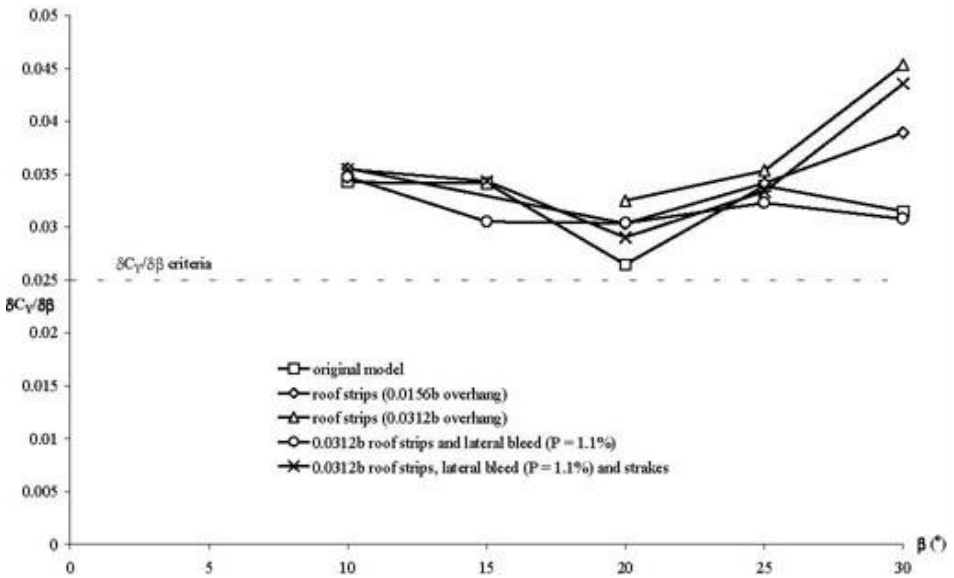

Figure 23. Effect of roof strips, lateral bleed and strakes on the rate of change in side-force with yaw angle. α = 0.5°, hc = 0.1b

Infographic on aerodynamic stability

Numerical and Experimental Aerofoil Evaluation

Mesh convergence study

To study the effects of mesh convergence, we are analysing the different results obtained when simulating the aerofoil with an AoT of 0 degrees with a range of meshes, augmenting the total amount of cells between iterations. The wing was tested in a positive lift coefficient generation position.

0 degrees Angle of Attack	Cells	Faces	Vertices
Mesh 1	2,382	4,615	2,529
Mesh 2	8,535	16,777	8,827
Mesh 3	38,155	75,180	39,283
Mesh 4	88,087	173,890	90,370
Refined mesh	152,807	303,328	155,093

Table 5. Mesh creation results

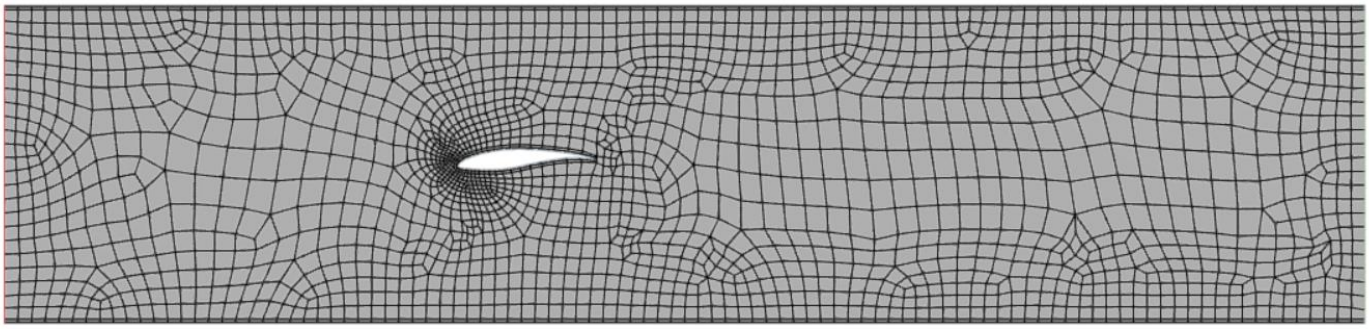

Figure 24. First mesh iteration used for mesh convergence and wall modelling study

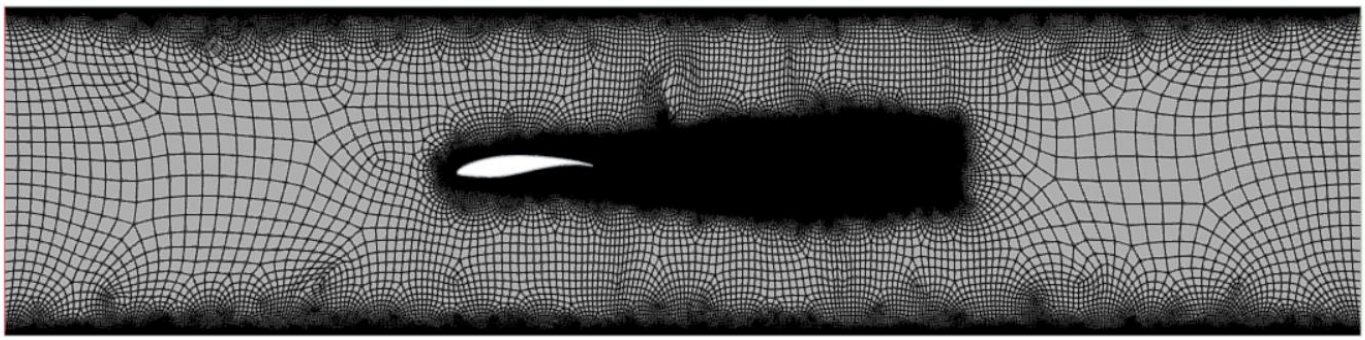

Figure 25. Final refined mesh used for mesh convergence and wall modelling study

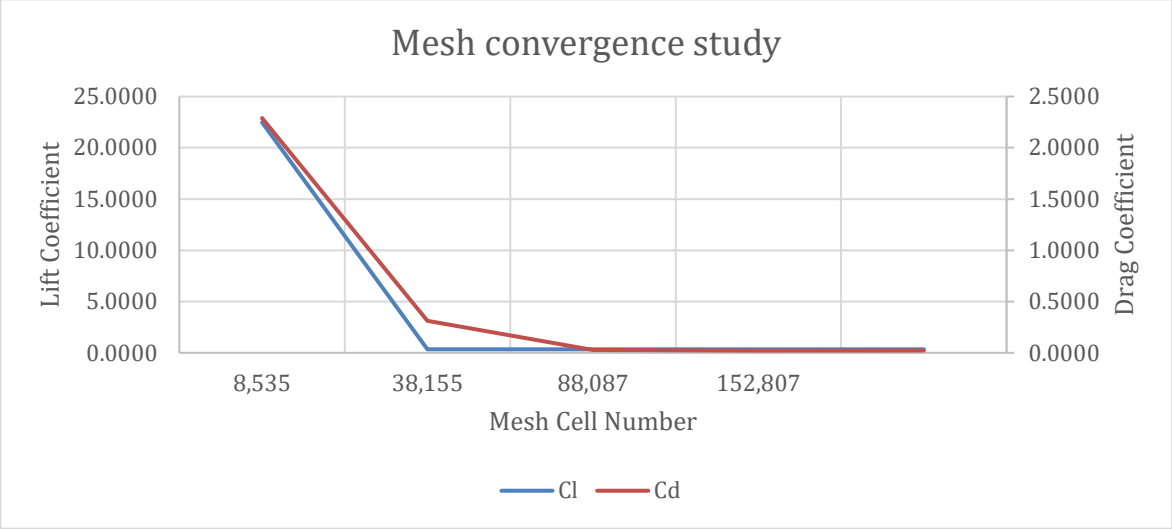

Figure 26. Mesh convergence study results

From the results obtained, we can observe a different convergence point for the lift coefficient and the drag coefficient, achieving first the lift convergence at approximately 30,000 cells, against the almost 90,000 cells needed to converge the drag coefficient.

This difference in convergence suggests to us that the lift is not that sensitive to flow characteristics compared to drag, which needs a more refined wake in order to obtain accurate measurements.

0 degrees Angle of Attack	Cl	Cd
Experimental data	0.3492	0.0159
Mesh 1	22.4768	2.2901
Mesh 2	0.3564	0.3129
Mesh 3	0.3527	0.0279
Mesh 4	0.3431	0.0227
Refined mesh	0.3438	0.0227

Table 6. Correlation between meshes iterations and experimental results

The difference in drag coefficient can be attributed to the wake flow, as the aerofoil used for the CFD simulations has a square trailing edge, disturbing the flow and equalisation of pressures at the wing outlet.

Effects of Wall Y+ modelling

To study the effects of wall modelling, the same meshes as in the previous study are used:

- Unrefined meshes: The prism layers number, thickness and stretching have not been modified, only base size, target surface size and minimum surface size where decreased.
- Refined mesh: The base size, target surface size and minimum surface size where further decreased, the number of prism layers has been increased, the thickness has been decreased and the stretching has been left unchanged, in order to improve the boundary layer readings on the aerofoil while achieving a low computational cost.

Optimizing Y+ values improve the quality of data obtained in the boundary layer regarding lift and drag. A Y+ value bellow 1 is considered good for accurate data retrieval in 2D meshing.

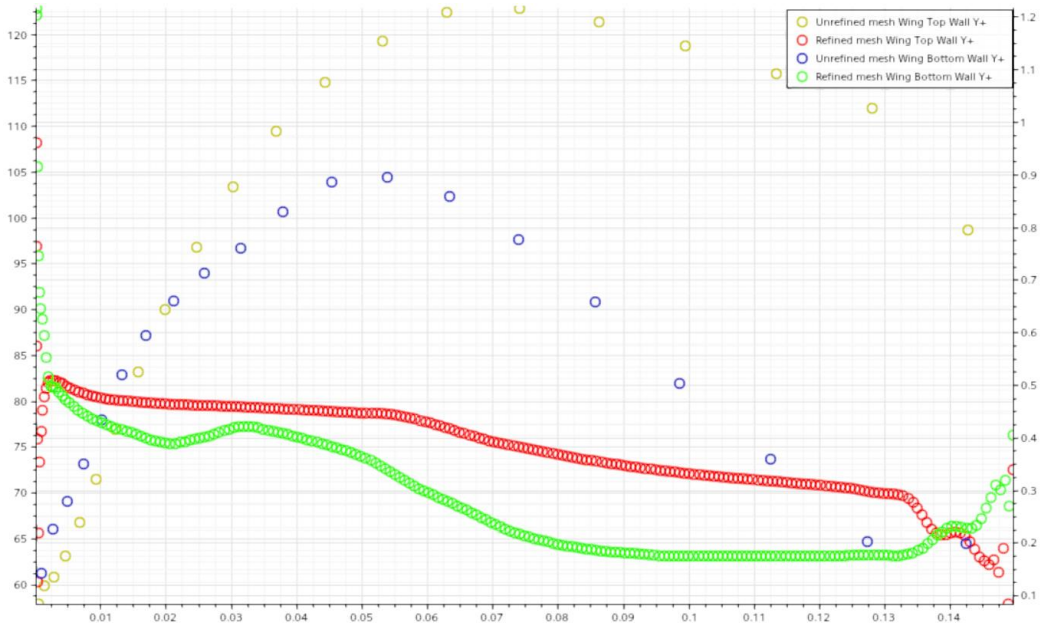

Figure 27. Y+ coefficient comparison between unrefined and refined mesh

Wall Y+ for the unrefined mesh is displayed on the left column, while refined mesh is on the right.

We can see that, for the refined mesh, we are able to obtain more data points because of the higher cell density, this also leads to lower Y+ values, which allows for accurate data retrieval.

For the unrefined mesh, data point density is much lower, as cell size is bigger. We can also observe much higher Y+ values, which indicates that the mesh is inaccurate for data retrieval.

Numerical and Experimental force and pressure coefficients correlation

For the refined mesh, we evaluate both the force and pressure coefficients from 0 to 16 degrees of AoT in 2-degree increments, comparing the results found in the CFD analysis to the experimental values. The aerofoil was tested a 3-degree offset opposite to the AoT growth for the 0-degree AoT.

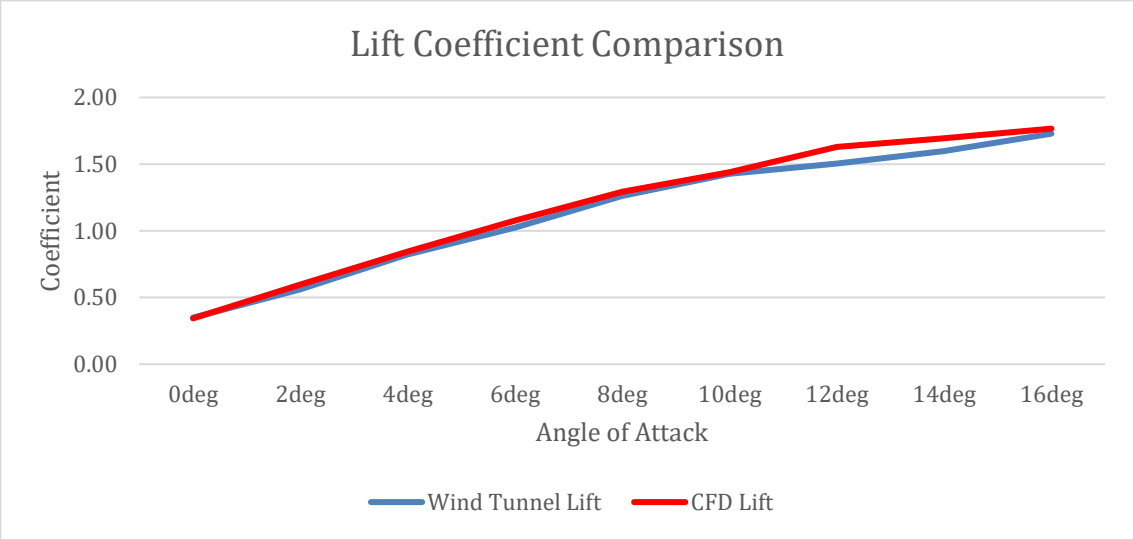

Figure 28. Lift coefficient comparison between experimental and CFD results

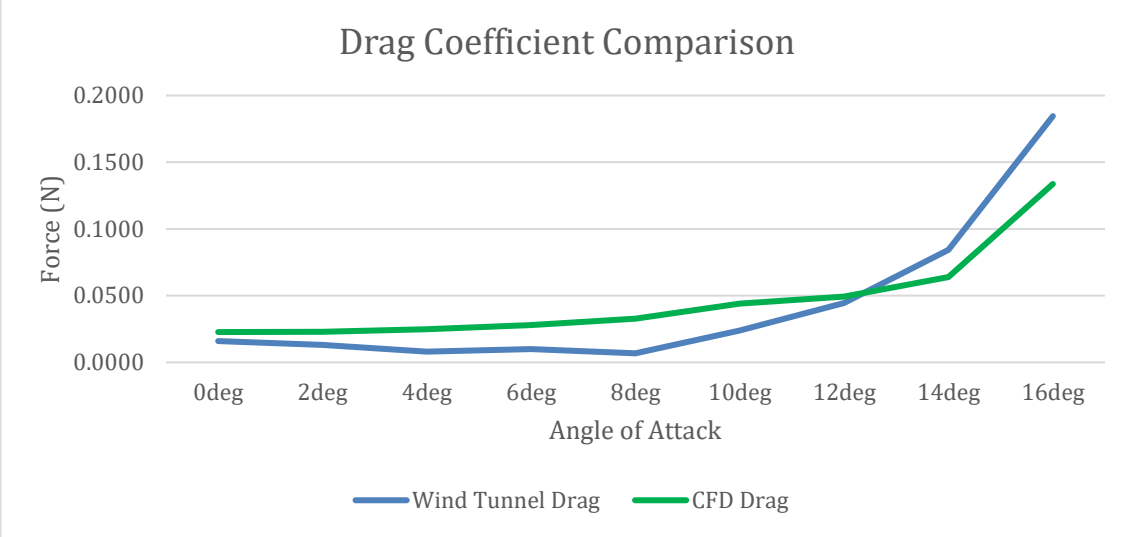

Figure 29. Drag coefficient comparison between experimental and CFD results

Although we can observe a close correlation between the Cl, we can observe a slight variation on Cd, this is due to the mesh needing to be more refined, as well as the CAD model needing refining to include a trailing edge. We can observe that the optimum AoT for the wing in both experimental and CFD is 8 degrees, as the aerofoil produces the best Cl/Cd ratio.

To compare the pressure coefficients, we need to obtain those achieved on the experimental analysis, making use of the formula (Barnard, 2001):

$$C_p = \frac{P - P_{Free\ Stream}}{\frac{1}{2} * \rho * V^2_{Free\ Stream}}$$

Once calculated, we import them into Star CCM+ to compare them with the results achieved by CFD:

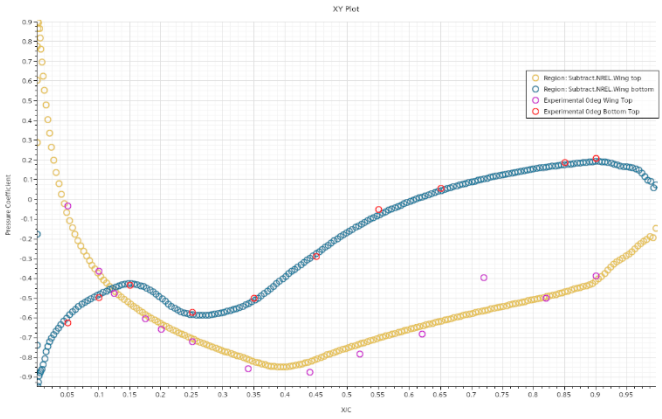

Figure 30. 0-degree AoT pressure coefficient comparison

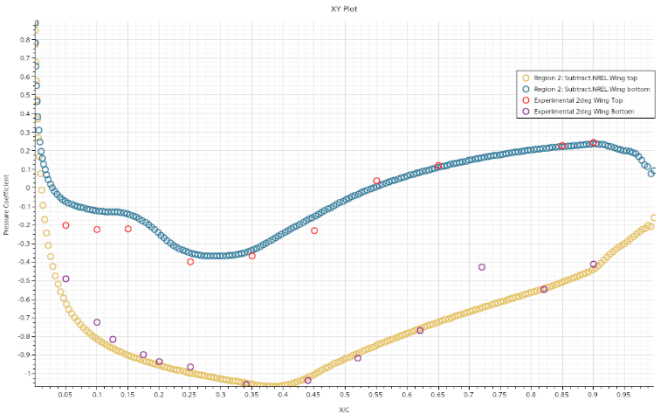

Figure 31. 2-degree AoT pressure coefficient comparison

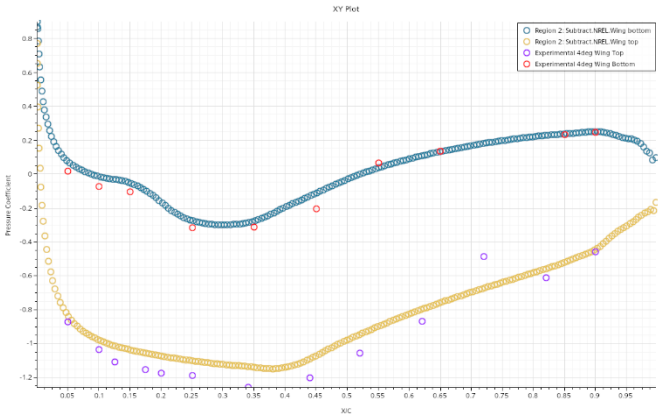

Figure 32. 4-degree AoT pressure coefficient comparison

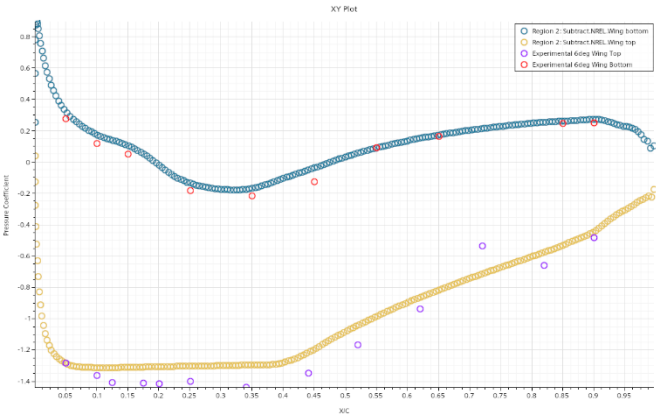

Figure 33. 6-degree AoT pressure coefficient comparison

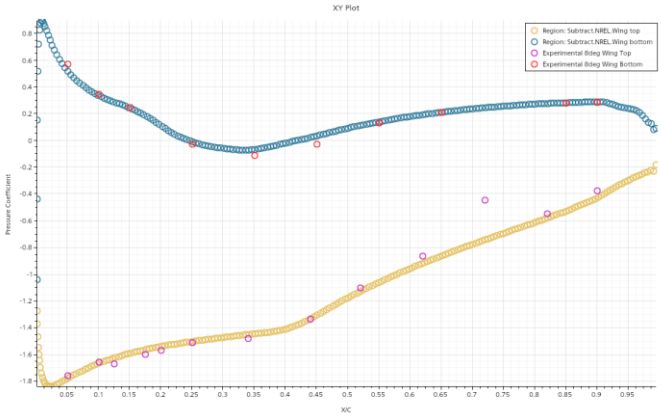

Figure 34. 8-degree AoT pressure coefficient comparison

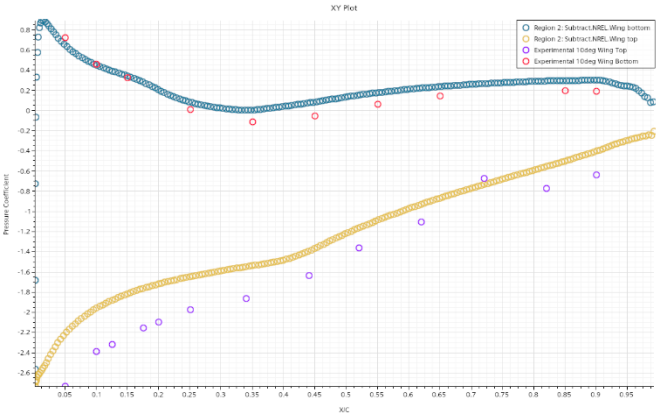

Figure 35. 10-degree AoT pressure coefficient comparison

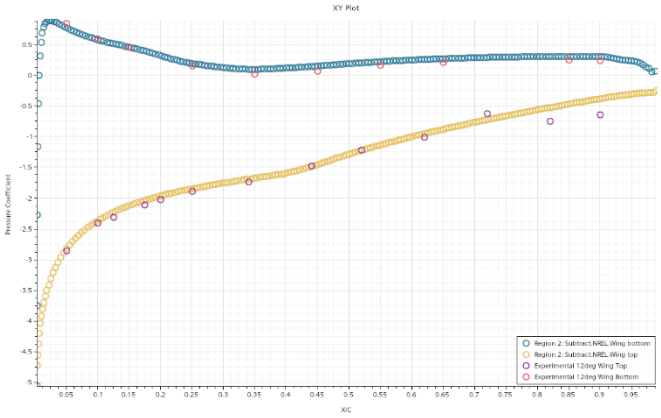

Figure 36. 12-degree AoT pressure coefficient comparison

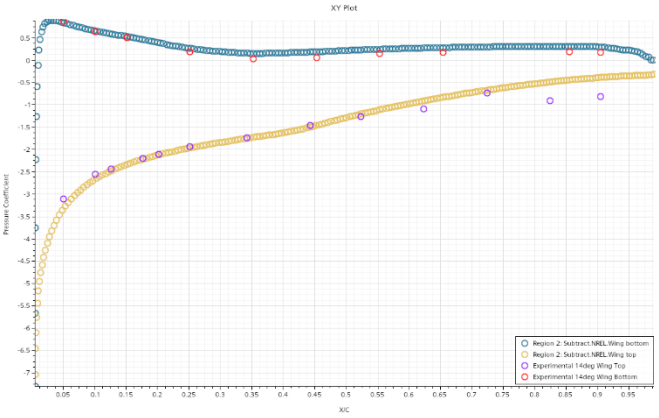

Figure 37. 14-degree AoT pressure coefficient comparison

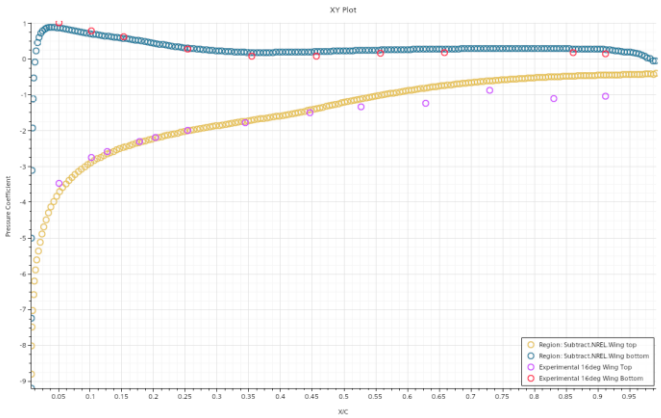

Figure 38. 16-degree AoT pressure coefficient comparison

We can observe that the correlation between pressure coefficients from the wind tunnel and the CFD is high, increasing the correlation as the AoT increases.

We can also observe that pressure coefficient at the leading-edge increases as the AoT increases, due to the higher air stagnation, as well as the pressure coefficient at the trailing edge maintaining a similar coefficient, due to the air reaching near free-stream conditions.

Personal reflection

During the completion of this portfolio, I have seen my understanding of aerodynamic concepts and their impact on vehicle performance and stability improve greatly and rapidly.
Through analysing the theoretical impact of different forces and bodywork on vehicle performance and stability, I have gained an insight into what an engineer should focus on improving depending on the use case of the vehicle. The effect of yaw on vehicle performance and stability has also been made very relevant to me by studying the principles on which both topics are based. The evaluation of the boundary layer present in the OBU wind tunnel allowed me to understand some of the correct practices that should be considered when conducting experiments in a wind tunnel, as I was able to observe and understand the effects of the correct placement of the test object on obtaining accurate data.

The practical part of the portfolio, where I analysed an aerofoil in CFD was of great use and interest to me, as I had no prior knowledge of CFD analysis and this exercise helped me gain knowledge of good practice and evaluation of results, as well as gaining confidence in the correlation between CFD results and real-world results.

Reflecting on the work done, I think that, although all the bases requested are covered, some explanations may be a little brief.

Finally, some aspects I wish I could have added to the portfolio would be a proper CFD analysis of the effect of yaw and different types of bodywork on vehicle performance, as well as including a more detailed section on optimising the computational cost-to-performance ratio for CFD simulations.

References

Milliken, W.F. and Milliken, D.L. (1995) Race Car Vehicle Dynamics. Warrendale, PA: SAE International.

Hucho, W.H. (2013) Aerodynamics of Road Vehicles: From Fluid Mechanics to Vehicle Engineering. 5th edn. Warrendale, PA: SAE International.

Howell, J. (2015) 'Aerodynamic drag of passenger cars at yaw', SAE Mobilus. Available at: https://saemobilus.sae.org/articles/aerodynamic-drag-passenger-cars-yaw-2015-01-1559#view

Abe, K., Ohya, Y., and Tominaga, Y. (1993) Computational Wind Engineering 1. Amsterdam: Elsevier. Available at: https://www.sciencedirect.com/book/9780444816887/computational-wind-engineering-1

Sagaut, P. (2018) Basics of Engineering Turbulence, 2nd edn. Amsterdam: Elsevier. Available at: https://www.sciencedirect.com/book/9780128039700/basics-of-engineering-turbulence

Fujihashi K. and Okumura K. (2000) 'Analysis of vehicle stability in crosswinds', SAE Technical Paper. Available at: https://saemobilus-sae-org.oxfordbrookes.idm.oclc.org/papers/analysis-vehicle-stability-crosswinds-2000-05-0255

John, M., et al. (2018) 'Experimental and Numerical Study of the DrivAer Model Aerodynamics´, SAE Technical Paper. Available at: https://doi-org.oxfordbrookes.idm.oclc.org/10.4271/2018-01-0741

Wieser, D., et al. (2014) 'Experimental Comparison of the Aerodynamic Behavior of Fastback and Notchback DrivAer Models', SAE Technical Paper. Available at: https://doi-org.oxfordbrookes.idm.oclc.org/10.4271/2014-01-0613

Dominy R., Ryan A., and Sims-Williams D.(2000) 'Aerodynamic stability of a Le Mans prototype race car in off-design pitch conditions', SAE Technical Paper. Available at: https://saemobilus-sae-org.oxfordbrookes.idm.oclc.org/papers/aerodynamic-stability-a-le-mans-prototype-race-car-off-design-pitch-conditions-2000-01-0872#view

Tingalls, C. (2020) 'What is convergence in CFD?', Medium. Available at: https://medium.com/@christophertingalls/what-is-convergence-in-cfd-5a0c7ab5efa9#:~

=CFD%20simulations%20involve%20solving%20complex,has%20reached%20a%20stable%20state

Skill-Lync (2023) 'CFD: All about the convergence criteria', Skill-Lync. Available at: https://skill-lync.com/blogs/technical-blogs/cfd-all-about-the-convergence-criteria

Ghmati, R., et al. (2013) The Study of Wall Y+ of Incompressible Turbulent Flow Over High Lift Devices Using CutCell Meshing. SAE Technical Paper 2013-01-1402. Available at: https://doi-org.oxfordbrookes.idm.oclc.org/10.4271/2013-01-1402

Gómez-Cortés, P., Al-Kayiem, H.H., and Arifin, A. (2024) 'Numerical investigation on ...', Applied Thermal Engineering, 215, p. 122678. Available at: https://doi.org/10.1016/j.applthermaleng.2024.122678

Varney M., et al. (2020) 'Experimental data for the validation of numerical methods: drivAer model´. Loughborough University. Available at: https://hdl.handle.net/2134/14784513.v1

Durbin, P.A. (2018) 'Chapter 12 - Turbulence modeling: an overview', in Advanced Fluid Mechanics. Amsterdam: Elsevier. Available at: https://www.sciencedirect.com/science/article/abs/pii/B9780128179499000128

Wilcox, D.C. (2010) 'Chapter 8 - Turbulence effects and modeling', in Basic Fluid Mechanics. Oxford: Butterworth-Heinemann. Available at: https://www.sciencedirect.com/science/article/abs/pii/B9780080966328000084